Phase-transition behavior in the random-field antiferromagnet $Fe_{0.5}Zn_{0.5}F_2$

J. P. Hill
Department of Physics, Brookhaven National Laboratory, Upton, New York 11973

Q. Feng, Q. J. Harris, and R. J. Birgeneau
Department of Physics, Massachusetts Institute of Technology, Cambridge, Massachusetts 02139

A. P. Ramirez
AT&T Bell Laboratories, 600 Mountain Avenue, Murray Hill, New Jersey 07974

A. Cassanho*
Center for Materials Science and Engineering, Massachusetts Institute of Technology, Cambridge, Massachusetts 02139
(Received 26 April 1996)

We present a combined magnetic x-ray and neutron scattering study of the order parameter of the diluted antiferromagnet $Fe_{0.5}Zn_{0.5}F_2$ in an applied field. This system is believed to be modeled by the three-dimensional random-field Ising model. A long range ordered (LRO) state is prepared through a zero-field-cooled procedure (ZFC). The evolution of this LRO state is studied on warming at fixed field. The x-ray order parameter data are well described by a power-law-like transition at all fields with an exponent β_{ZFC} varying from 0.21 to 0.12. The transition region is broadened and may be described by a Gaussian distribution of transition temperatures, centered at $T_C(H)$, of width $\sigma_{\mathrm{ZFC}}(H)$. It is found that $\sigma_{\mathrm{ZFC}}(H)=AH^2+B$. This rounding is attributed to anomalously slow dynamics, which prevents equilibrium being attained for experimentally relevant time scales for $T<T_M(H)$ where $T_M(H)$ is the temperature below which metastability effects occur. The apparent critical behavior in fact represents a continuous evolution from metastable behavior towards equilibrium behavior. Neutron scattering studies on the same sample allow identification of $T_C(H)$ with the temperature at which the correlation length of the zero-field-cooled fluctuations reaches a maximum value, equal to the corresponding field-cooled value. A qualitative finite size scaling argument is presented to explain the H^2 width dependence. Data showing similar scaling of the width of the ZFC transition region inferred from the temperature derivative of the uniform magnetization as measured by superconducting quantum interference device magnetometry and from neutron scattering measurements of the pseudocritical scattering are also presented. These results lead to an interpretation of indirect specific heat measurements in which the ZFC peak structure, previously attributed to critical fluctuations, is seen instead to arise entirely from a LRO contribution to the measured quantity. [S0163-1829(97)03501-7]

I. INTRODUCTION

The problem of disorder and its role in critical phenomena has received considerable attention over the past two decades. Motivation to study this problem has been twofold. First, quenched disorder in the form of frozen impurities or defects is almost unavoidable in any real system and must therefore be understood in any complete theory of phase transitions. Second, the problem has proven to be remarkably complex, displaying a rich variety of new phenomena.

The random-field Ising model (RFIM) is believed to capture the essential physics for many systems with discrete symmetry. In this model, disorder is introduced through a site random variable h_i, which couples linearly to the order parameter,

$$\mathcal{H}=\sum_{\langle ij\rangle} J_{ij}S_i^zS_j^z-\sum_i h_iS_i^z, \tag{1}$$

and averages to zero, with finite variance, $\langle h_i\rangle=0$, $\langle h_i^2\rangle\neq 0$. It is generally believed that in equilibrium the long range ordered (LRO) ground state is not destroyed by the presence of weak, frozen random fields (h_i), provided that the spatial dimension is greater than 2, that is, the lower critical dimension of the RFIM is $d_{\mathrm{LCD}}=2$.[1,2] The critical behavior of the model is still not well understood. This is largely because metastability effects greatly hamper the experimental and numerical investigation of the equilibrium properties. In this work, we address the origin and nature of the metastability.

The random-field Ising model is most simply realized by applying a uniform external magnetic field to a randomly diluted antiferromagnet.[3–5] Experiments on diluted antiferromagnets have shown that, on cooling in a random field (FC), the system abruptly drops out of equilibrium at a well defined temperature and never achieves long range order (LRO). Rather it forms a short range ordered (SRO) domain state.[6] If the system is zero field cooled (ZFC) and a random field subsequently turned on however, LRO is retained. Villain[7] and Fisher[8] (VF) independently proposed that the metastability in the RFIM originates in the complex structure of the free energy. There are many minima in the free energy, which correspond to rearrangements of the domain walls. At long length scales the static random-field fluctuations dominate over the usual dynamic thermal fluctuations[9]

and in general, these minima are well separated. The Villain-Fisher picture is as follows. For a given correlated volume, there is only one thermally populated minimum. Thermal fluctuations in this minimum are small because of the steep curvature in the free energy.[8] However, on rare occasions, with probability T/ξ^{θ} two minima occur within a correlated volume which differ in energy only by order T. In such cases, the equilibrium fluctuations may be thermally activated over the free energy barrier. To achieve such a reversal of a block of spins of size R, a free energy barrier of height $\omega(R)\approx R^{\theta}$ must be overcome. R^{θ} is the random-field energy of a volume R^{d} (the surface tension vanishes as $T\rightarrow T_C$) and θ is the exponent which modifies the hyperscaling relation to $(d-\theta)\nu=2-\alpha$. Arrhenius' law then implies that the characteristic relaxation time of the system close to the transition, that is, the time to flip a correlated volume, is

$$\tau\approx\tau_0\exp(C\xi^{\theta}), \tag{2}$$

where τ_0 and C depend on the random field strength. The ''activated dynamics'' of Eq. (2) result in extreme critical slowing down and the system cannot equilibrate on experimentally accessible time scales, as $\xi\rightarrow\infty$. The anomalously slow dynamics at the transition complicate experimental and numerical investigations of the critical behavior. While it is clear that the dynamics at the transition are slow, it is difficult to verify the ideas of VF in detail. In particular, data over many decades of frequency are needed to distinguish Eq. (2) from conventional critical slowing down, $\tau\sim\tau_0\xi^{z}$.[10,11] An alternative test is to investigate the field dependence of the dynamic rounding produced by Eq. (2). This is one of the goals of the work reported in this paper. For RFIM systems with a conserved order parameter, such as binary fluid mixtures in random media, Huse has shown[12] that activated dynamics are also present at length scales smaller than a dynamic crossover length. This crossover length diverges as the transition is approached.

In this paper, we report the results of a study of the disordering of the RFIM as realized in the site-diluted antiferromagnet $Fe_{0.5}Zn_{0.5}F_2$. We have investigated the loss of LRO on warming a ZFC LRO state through the metastability boundary. Although the ZFC state has LRO, it is not the equilibrium ground state of the RFIM because an artificially high degree of order has been frozen in by the ZFC procedure. Were it possible to remain in equilibrium on FC, the resulting LRO state would have significantly more disorder than the ZFC state since some patches of spins would follow their local random fields, despite the presence of a backbone of LRO. Nevertheless, by studying the transition out of this metastable LRO state it is possible to gain insight into the disordering mechanism and in turn shed light on the problem of hysteresis in this system.

By combining the complementary techniques of magnetic x-ray scattering and neutron scattering, we have obtained reliable measurements of the order parameter and of the diffuse scattering. The ZFC order parameter is seen to decay to zero with increasing temperature through a rounded power-law-like transition. This is well described by a Gaussian distribution of transition temperatures with a width approximately proportional to the applied field squared. The center of the distribution coincides, within errors, to the temperature at which the correlation length associated with the diffuse scattering reaches its maximum. In addition, superconducting quantum interference device (SQUID) magnetometry measurements of the uniform magnetization were made which also show a $\sim H^2$ broadening of the ZFC transition in quantitative agreement with the x-ray and neutron results. Our results qualitatively confirm the ideas of Villain and Fisher.[7,8] However, as we shall discuss below, understanding the H^2 broadening requires further theoretical development.

The paper is organized as follows. Following a brief survey of previous experimental work in Sec. II, we discuss the sample preparation and the experimental procedures used in this experiment in Sec. III. In Sec. IV, we first present x-ray measurements of the ZFC order parameter and the observed magnetic field dependence of the transition width. These data, in conjunction with neutron scattering measurements of the diffuse scattering, provide a picture of the transition occurring through the flipping of successively larger blocks of spins. The divergence of the size of the flipped regions saturates at a finite value, equal to the corresponding field-cooled value, for experimentally relevant time scales, due to the extreme critical slowing down. This has the effect of rounding the transition in a manner analogous to finite size broadening. Measurements of the thermal derivative of the uniform magnetization also provide information on the transition region. Again, an H^2 dependence of the width of the transition region is found. In Sec. V, we discuss the results and derive an empirical scaling law for the transition width based on finite size arguments. We then apply the ideas developed in this work to other techniques, specifically indirect specific heat measurements, which had previously been interpreted as reflecting a critical contribution on ZFC, in apparent contradiction with the scattering results presented here. We show that in fact the ZFC-FC hysteresis of these measurements may arise solely from a LRO contribution, and successfully model magnetization and birefringence ZFC data with the x-ray intensity scaling function.

A preliminary report of some of the results and ideas presented here has recently been published.[13]

II. A BRIEF REVIEW OF PREVIOUS EXPERIMENTAL WORK

The Hamiltonian of Eq. (1) has been applied to a number of experimental systems, including adsorbed monolayers on a square substrate, two component fluids in random media, and certain Jahn-Teller systems. Systematic studies of the effects of random fields are impractical in these systems because the random-field strength cannot be easily varied. However, random fields conjugate to the order parameter are generated in random antiferromagnets by applying a uniform external field.[3–5] Hence a continuous variation of the random field is possible in these systems. Diluted Ising-like antiferromagnets including $Mn_{1-x}Zn_xF_2$, $Co_{1-x}Zn_xF_2$, and $Fe_{1-x}Zn_xF_2$ have therefore been the subject of much study over the past decade (for reviews see Refs. 14–17). A variety of experimental techniques have been used including neutron scattering,[18,19,6,20–24] optical birefringence and Faraday rotation,[21,25–29] dilatometry,[30,31] ac susceptibility,[10,11] SQUID magnetometry,[32,33] NMR techniques,[34] and more recently magnetic x-ray scattering.[13,35–38]

Broadening of the ZFC transition with increasing applied field was initially observed in the thermal expansion measurements of Shapira *et al.*,[31] and subsequently with a range of techniques.[25–28,39] Following the ideas of Villain[7] and Fisher[8] this broadening has been interpreted as being symptomatic of the extremely slow dynamics at the transition. ac susceptibility studies over seven decades of frequency[10,11] provided direct evidence of slow dynamics consistent with Eq. (2). In addition, Monte Carlo simulations have also observed strongly divergent correlation times consistent with activated dynamics (see, for example, Ref. 40). The apparent width of the transition, ΔT around $T_N(H)$, observed with measurements at frequency ω, is expected to scale as $\Delta T \sim |\ln\omega|^{-1/\theta\overline{\nu}}$, where $\overline{\nu}$ is the RFIM correlation length exponent. Ramos *et al.*[26] argued that the crossover from the $H=0$ T REIM fixed point causes the scaling behavior to be modified to $\Delta T \sim h_{\mathrm{RF}}^{2/\phi}[\ln(\omega h_{\mathrm{RF}}^{-2\nu z/\phi})]^{-1/\theta\nu}$, where ν and z are the REIM correlation length and dynamical critical exponents, respectively.

A few workers have attempted to quantify the field dependence of the broadening. In a neutron scattering study, Belanger *et al.*[22] found the broadening varied as $H^{2/\phi}$ with $\phi=1.42$ for $H\leqslant 3.0$ T in $Fe_{0.46}Zn_{0.54}F_2$. Similarly optical Faraday rotation data of Pollack *et al.* on $Fe_{0.47}Zn_{0.53}F_2$ (Ref. 27) taken at four fields obeyed a $H^{2/\phi}$ power law with $\phi=1.49\pm0.1$. Magnetic x-ray scattering data showed that the broadening of the transition in $Mn_{0.75}Zn_{0.25}F_2$ followed an H^2 field dependence[36] up to $H=7.0$ T. In this latter work, it was shown that the broadened transition was centered around a temperature $T_C(H)$ where $T_C(H)>T_N(H)$.

III. EXPERIMENTAL DETAILS

FeF_2 has the rutile-type structure, with the spins oriented along the c axis. It orders antiferromagnetically below the Néel temperature $T_N=77$ K. A large single ion anisotropy makes this an excellent example of a three-dimensional (3D) Ising system.[41]

The samples of $Fe_{0.5}Zn_{0.5}F_2$ used in this work were grown at MIT using the Czochralski method, from a 50% FeF_2, 50% ZnF_2 initial mix. The growth direction was along the a axis. The lattice constants are $a=4.71$ Å and $c=3.24$ Å. A disk shaped slice was cut from the boule, of diameter 20 mm and thickness 3 mm. A flat face, parallel to the (200) planes and perpendicular to the growth direction was polished with 0.05 μm grit for the x-ray work. It was discovered that one-quarter of the disk had a narrower mosaic and this piece was cut away and used for both the x-ray and neutron scattering experiments. The mosaic width of the (200) reflection was 0.012°, full width at half maximum (FWHM) as measured with x rays. A small concentration gradient was present across the boule, along the (200) growth direction. Across the 3 mm slice this small gradient is manifest as a slight rounding of the $H=0$ T transition in the neutron scattering data. In Fig. 1(a), we plot the neutron peak intensity at the (100) magnetic Bragg peak position in zero field. Our results confirm that this rounding is less than 0.2 K and thus is significantly smaller than the broadening seen under an applied field, which is the subject of this work. For the x-ray experiments, the effect of any concentration gradient is further reduced due to the small penetration depth of the x rays,

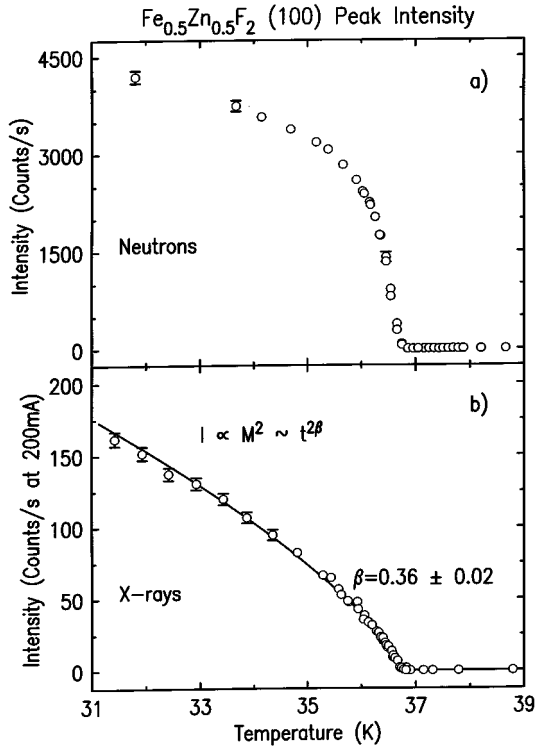

FIG. 1. X-ray and neutron peak intensity at the (100) magnetic reciprocal lattice point in zero field. (a) The neutron peak intensity. The intensity at low temperatures is modified by extinction effects and a reliable determination of the order parameter is not possible. (b) The x-ray peak intensity. The intensity is directly proportional to the sublattice magnetization squared. The solid line is the result of a least squares fit to a single power law with $\beta=0.36\pm0.02$. The theoretically predicted value is $\beta=0.35$ (Ref. 42).

~ 3.7 μm. This is evidenced by the sharpness of the zero-field transition shown in Fig. 1(b). The x-ray data exhibit a rounding of less than 0.15 K (FWHM) which requires that any variations in the concentration, Δx, be $\Delta x \leqslant 2\times10^{-3}$ over the illuminated volume. Concentration gradients will also introduce an additional rounding at field, due to the dependence of the random-field transition temperature shift on the dilution. However, this is small compared to the zero-field effects.[36] Furthermore, our measurements of the broadening observed in the quantity (dM/dT) (see Sec. IV B) agree quantitatively with identical measurements performed by Lederman *et al.*,[33] on a crystal of $Fe_{0.46}Zn_{0.54}F_2$ with a quoted concentration gradient of only 0.5%/cm. We conclude that the results reported here are not significantly influenced by any concentration gradient effects.

The x-ray scattering experiments were performed at the MIT-IBM X20 beamlines at the National Synchrotron Light Source. The zero-field experiments were carried out in a closed cycle helium cryostat mounted on a six circle diffractometer at X20C and the experiments in an applied field were performed at X20A. These beamlines have been described in detail elsewhere[36] and will not be discussed further. The experiments in an applied field utilized an x-ray compatible 10 T superconducting magnet. The sample was mounted with the c-axis vertical, parallel to the applied field. Temperature control was achieved via a carbon glass resistor

and was stable to <10 mK during the course of a typical scan. The diffraction geometry was horizontal, with a longitudinal resolution of 4×10^{-4} Å^{-1} HWHM. The transverse resolution was controlled by the sample mosaic and was 1×10^{-4} Å^{-1} HWHM. The vertical resolution was determined by collimating slits and was 5×10^{-3} Å^{-1} HWHM. X rays of energy $E=6.9$ keV were used.

The neutron scattering measurements were performed on spectrometers H7 and H8 at the Brookhaven High Flux Beam Reactor. The data were taken with the spectrometers in the double axis (energy integrating) mode with collimators of 10′-10′-sample-10′ unless otherwise stated. The resulting resolutions were 0.0037, 0.0014, and 0.088 Å^{-1} FWHM for the longitudinal, transverse, and vertical directions, respectively. The incident neutron wave vector was fixed at 2.67 Å^{-1} with a PG(002) monochromator. Pyrolytic graphite filters were used to remove higher harmonics. We note that throughout this paper the neutron data have been uniformly shifted in temperature by $\Delta T=-3.1$ K. This shift is made with the assumption that the observed difference in the $H=0$ T transition temperatures, as measured by the two techniques on the same sample, is the result of the differing thermometry in the two cryostats and can be simply corrected for. This assumption will be justified later in this paper when the neutron and x-ray data are directly compared. The zero-field transition temperature as determined by the SQUID measurements is in agreement with the x-ray work.

Measurements of the uniform magnetization were performed in a commercial SQUID magnetometer at MIT. This SQUID is capable of measurement at fields up to $H=5.5$ T and at temperatures down to 2.2 K. The data presented in Sec. IV were taken on a small piece of $Fe_{0.5}Zn_{0.5}F_2$ cut from the same boule as the x-ray and neutron sample. The c axis was aligned with the vertical field to within $\pm5°$. Misalignments within this range have negligible effects on the overall results. Sample temperatures were controlled to within ±0.01 K during the course of a measurement. At each temperature the sample was scanned through the measuring coils three times and the average moment calculated from the three runs.

IV. RESULTS

A. Scattering measurements of the staggered magnetization

Two strengths of magnetic x-ray scattering are (1) the small cross section, which allows an extinction free measurement of the order parameter and (2) the inherent high angular resolution of the synchrotron x-ray source. These two strengths are well matched to the problem of measuring the ZFC staggered magnetization.

Figure 1(b) shows the temperature dependence of the x-ray peak intensity at the (100) magnetic Bragg reflection, for $H=0$ T. The arrangement of the fluorine atoms results in chemical and magnetic unit cells of equal size. However, pure charge scattering is symmetry forbidden at the (100) position.[35] It is nonetheless possible for multiple charge scattering processes to produce scattering at the (100) position (for example $\mathbf{q}_{011}+\mathbf{q}_{1\,1\,\overline{1}}$ is allowed) and this is the major source of background in these experiments. Multiple scattering is minimized by rotating the sample about the scattering vector and by varying the incident x-ray energy until an optimal configuration is found. For the data shown in Fig. 1(b), and all subsequent data, a temperature independent multiple scattering background of ~10 counts s^{-1} has been subtracted. This is a significantly larger background than that achieved in the $Mn_{0.75}Zn_{0.25}F_2$ experiments.[35–37] We attribute this partly to the larger sample mosaic in the present case (0.012° cf. 0.004°) which has the effect of making the Ewald sphere less well defined.

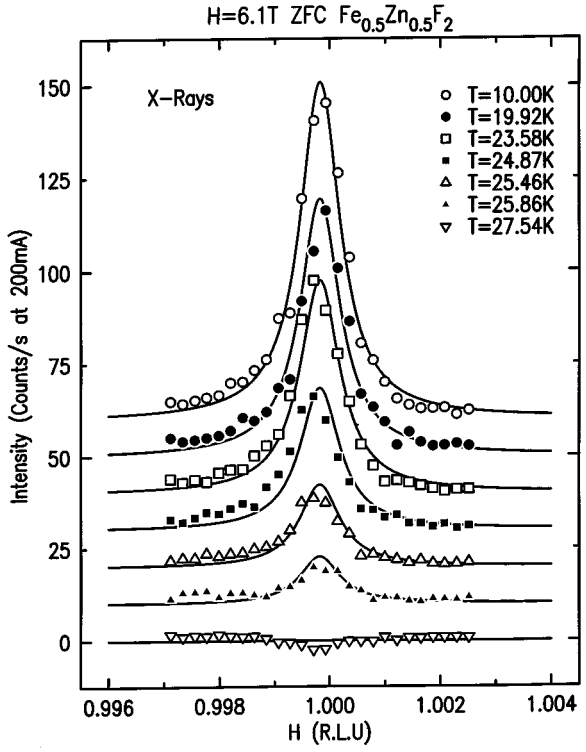

FIG. 2. Representative longitudinal x-ray scattering scans. Data were taken at $H=6.1$ T on warming, following a ZFC procedure. The solid lines are the results of least squares fits to Lorentzians of constant width, equal to 4×10^{-4} reciprocal lattice units.

The observed x-ray line shape at the (100) position is resolution limited at all temperatures and hence the peak intensity is proportional to the integrated intensity and to the square of the staggered magnetization. The solid line in Fig. 1(b) is the result of a least squares fit to a power law $I\sim(1-T/T_N)^{2\beta}$ with $T_N=36.7\pm0.08$ K and $\beta=0.36\pm0.02$. This value of T_N is 48% of the Néel temperature of FeF_2, $T_N(x=0)=77$ K. The observed value of β agrees to within the errors with the theoretical value for the random exchange Ising model (REIM) $\beta_{\rm th}=0.35$.[42]

We now consider the data taken in a nonzero field. The ZFC state is first prepared by cooling in zero field to 10 K, then raising the field to the desired value. The resulting (100) magnetic peak was found to be resolution limited for all fields studied, corresponding to LRO with an antiferromagnetic domain size in excess of 1 μm. The temperature was then raised holding the field fixed. Scans at each temperature took approximately 30 min in the transition region with an additional 10 min thermal equilibration time. In Fig. 2, representative longitudinal scans, at a few selected temperatures from the $H=6.1$ T ZFC data set, are shown. The solid lines are one-dimensional Lorentzians of constant width, equal to

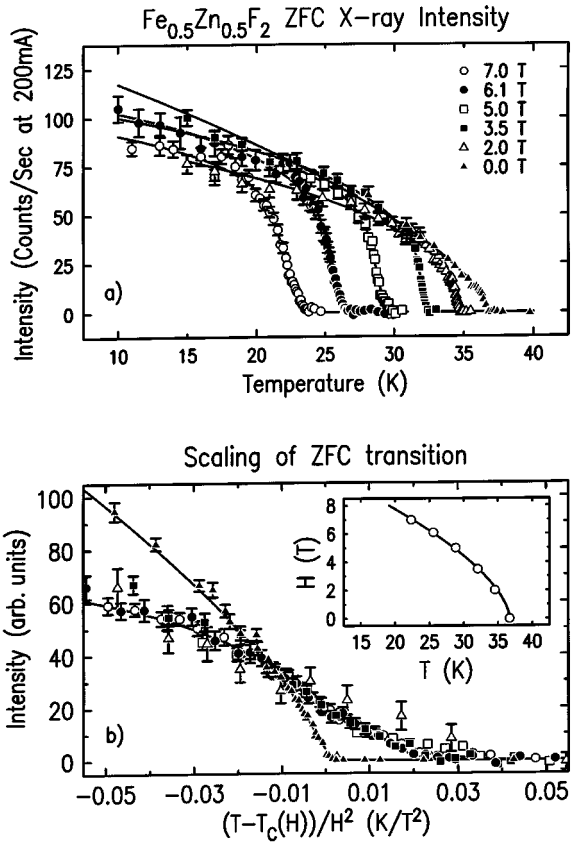

FIG. 3. (a) The ZFC order parameter squared as measured at the (100) position with x rays for five fields and $H=0$ T. For $H\neq 0$, the data are well described by a power-law-like behavior with a broadened transition region. The broadening is modeled by a Gaussian distribution of transition temperatures of width $\sigma_{\mathrm{ZFC}}(H)\propto AH^2$ (see text). (b) The $H\neq 0$ data of (a) replotted as a function of the temperature interval away from $T_C(H)$ as measured in units of H^2. This illustrates the rounding of the transition which is attributed to nonequilibrium effects arising from extreme critical slowing down and the universal scaling behavior of the ''trompe l'oeil'' critical phenomena. The inset shows the phase boundary of $Fe_{0.5}Zn_{0.5}F_2$ as determined from the x-ray fits.

4×10^{-4} reciprocal lattice units (here and throughout this paper, 1 reciprocal lattice unit$=2\pi/a=1.334$ Å). The multiple scattering background was measured at a number of temperatures above the phase boundary. An average of these spectra was then subtracted from the raw data to obtain the data shown in Fig. 2. The slight negative tendency in the center of the highest temperature scan in Fig. 2 results from the difference between this average and the multiple scattering present in that particular scan. Figure 3(a) displays the (100) peak intensity obtained from a series of such scans, for five fields and $H=0$ T. In each case, the scattering remained resolution limited at all temperatures and no critical scattering was observed. As was the case for $Mn_{0.75}Zn_{0.25}F_2$,[37] all of the $H\neq 0$ data are well described by a power law with a Gaussian distribution of transition temperatures. We emphasize that this is a heuristic form which has not yet been justified by any formal theory. The solid lines in Fig. 3(a) are the result of least squares fits to the form

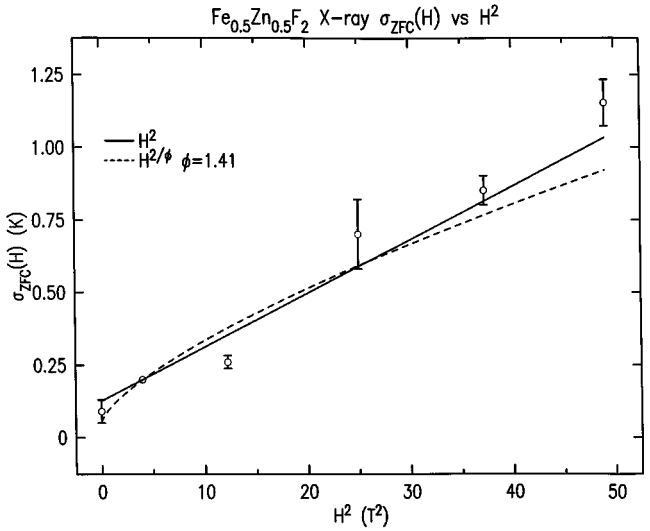

FIG. 4. The parameter $\sigma_{\mathrm{ZFC}}(H)$, which measures the observed x-ray ZFC transition width, plotted as a function of H^2. $\sigma_{\mathrm{ZFC}}(H)$ is extracted from the order parameter fits shown as solid lines in Fig. 3(a).

$$I(T,H)=\frac{1}{\sqrt{\pi\sigma_{\mathrm{ZFC}}^2(H)}}\int\left(\frac{t_c-T}{t_c}\right)^{2\beta}\times\exp\left[-\left(\frac{t_c-T_c(H)}{\sigma_{\mathrm{ZFC}}(H)}\right)^2\right]dt_c. \tag{3}$$

For $Mn_{0.75}Zn_{0.25}F_2$, $\sigma_{\mathrm{ZFC}}(H)$ was proportional to H^2 and this was also found to be the case in the present study of $Fe_{0.5}Zn_{0.5}F_2$. This field dependence of the width is shown in Fig. 4, where $\sigma_{\mathrm{ZFC}}(H)$ is plotted against H^2 (solid line). A straight line adequately fits the data. The dashed line represents a fit to $H^{2/\phi}$ behavior, with ϕ fixed to $\phi=1.41$. The goodness of fit parameter, χ^2, is about a factor of 2 worse for this fit. In the current work, we find β_{ZFC} has a slight field dependence, namely $\beta_{\mathrm{ZFC}}(2.0\ \mathrm{T})=0.21\pm0.03$, $\beta_{\mathrm{ZFC}}(3.5\ \mathrm{T})=0.16\pm0.03$, $\beta_{\mathrm{ZFC}}(5.0\ \mathrm{T})=0.13\pm0.03$, $\beta_{\mathrm{ZFC}}(6.1\ \mathrm{T})=0.12\pm0.03$, and $\beta_{\mathrm{ZFC}}(7.0\ \mathrm{T})=0.12\pm0.03$. The width is found to follow: $\sigma_{\mathrm{ZFC}}(H)=AH^2+B$ with $A=0.019\pm0.002$ K/T^2 and $B=0.12$ K. In $Mn_{0.75}Zn_{0.25}F_2$, the equivalent results were $\beta=0.2\pm0.05$ and $A=0.0034$ K/T^2. Holding the value of β_{ZFC} fixed at the average value$=0.15$ does not change the H^2 dependence of the transition width, but results in slightly worse fits to the order parameter data. The scaling of the data may be graphically illustrated by replotting the data of Fig. 3(a) and measuring the temperature difference from the center of the distribution in units of H^2. Such a plot is constructed in Fig. 3(b). The collapse of the data is excellent, illustrating that the H^2 dependence of the broadening is valid over a wide range of applied fields. We note that observation of this field dependence in $Fe_{0.5}Zn_{0.5}F_2$ rules out the possibility that the H^2 scaling in $Mn_{0.75}Zn_{0.25}F_2$ was a consequence of the weak anisotropy or the close proximity of a bicritical point in the latter system.

We note that very recently Wong,[43] utilizing an argument based on Fisher renormalization effects, has suggested that the underlying transition is in fact first order. The simplest form of a first order transition, namely $\beta_{\mathrm{ZFC}}\rightarrow 0$ in Eq. (3),

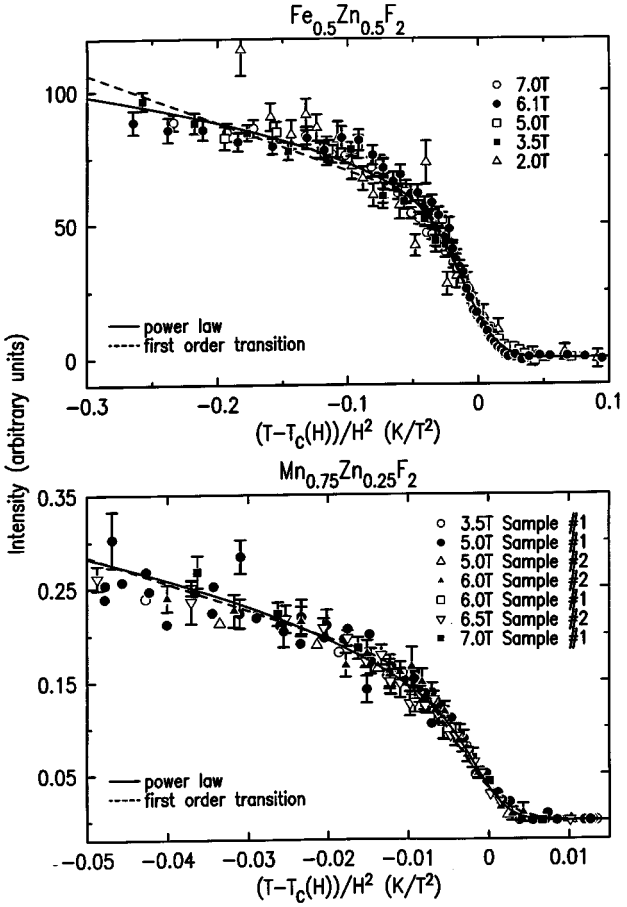

FIG. 5. Scaled magnetic Bragg intensity plotted as a function of $[T-T_c(H)]/H^2$ in $Fe_{0.5}Zn_{0.5}F_2$ and $Mn_{0.75}Zn_{0.25}F_2$. The solid and dashed lines are, respectively, the result of least squares fits to the power law and the first order models of the transition discussed in the text.

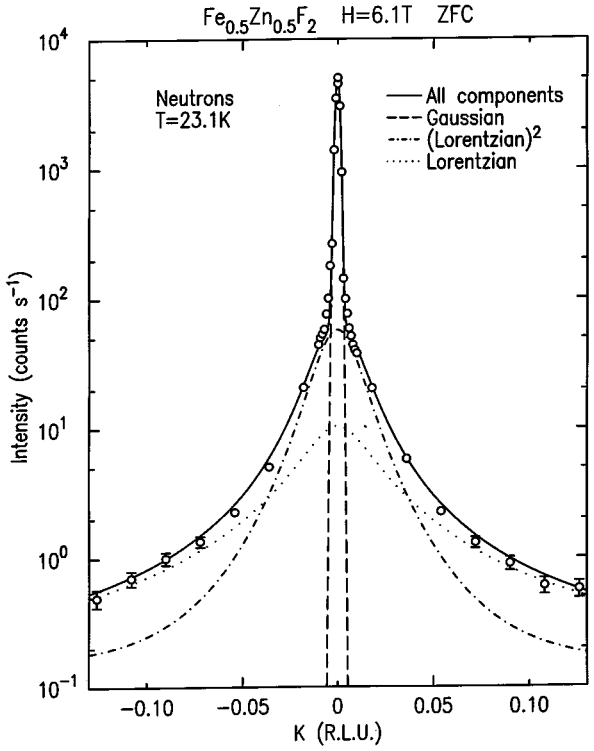

FIG. 6. A typical neutron scattering transverse scan through the (100) antiferromagnetic Bragg peak. The data shown were taken at $T=23.1$ K, $H=6.1$ T, following a ZFC procedure. The solid line is the result of a fit to the cross section discussed in the text, convolved with the 3D resolution function. The dotted, dot-dashed, and dashed lines illustrate the line shape components used in the fit.

does not fit our data. However, Wong pointed out that a mean-field transition, $\beta=1/2$, interrupted by a first order, discontinuous jump, and broadened by the same Gaussian distribution as Eq. (3), works well. In Fig. 5, we display the results of such fits for both the $Fe_{0.5}Zn_{0.5}F_2$ data of Fig. 3 and the $Mn_{0.75}Zn_{0.25}F_2$ data from our earlier work.[36] In each case, the solid line is the result of fit to the power law of Eq. (3) and the dashed line a fit to the first order model. Specifically, in the first order model, the first term of the integrand of Eq. (3) is replaced with $[1-(T/t^*(H))]$, for $T<t_c$, where $t^*(H)$ is the hypothetical temperature at which the mean field transition would occur were it not preempted by the first order jump. While the goodness of fits for the first order form are slightly larger than those of the power law, the data do not distinguish between the two models. Both models describe the ZFC transition region well, and both rest on plausible physical bases, although the Fisher renormalization argument only applies to diluted antiferromagnets in a field and the trompe l'oeil model is more general. In addition, the value for the parameter t^* obtained from the first order fits seems surprisingly large. We find $t^*=0.3\pm0.04$ K/T^2 for $Fe_{0.5}Zn_{0.5}F_2$ and $t^*=0.13\pm0.02$ K/T^2 for $Mn_{0.75}Zn_{0.25}F_2$ in the scaled units of Fig. 5. We conclude, however, that we cannot distinguish between these two approaches and that further experimental and theoretical work is necessary to gain a full microscopic understanding of the transition.

It is interesting to note that the transition is broadened significantly more in $Fe_{0.5}Zn_{0.5}F_2$ than was the case for $Mn_{0.75}Zn_{0.25}F_2$, at the same applied field. This difference arises from the larger random fields generated in $Fe_{0.5}Zn_{0.5}F_2$ by virtue of the greater dilution, and lower transition temperatures. In fact, $h_{\rm RF}^2$ is $\approx$4 times larger in the $x=0.5$ material at the same field. We will return to this point in Sec. V.

We next present neutron scattering results taken on the same sample of $Fe_{0.5}Zn_{0.5}F_2$. The data were taken in the double axis mode, thus the same-time correlation function is measured. The large cross section and broad resolution mean that the diffuse component resulting from the reversal of blocks of spins is observable in the ZFC state, in addition to the LRO. This diffuse component is observed to sharpen as the temperature is raised, reaching a maximum correlation length at $T_C(H)$. The two-axis data were fitted to the cross section,[18]

$$S(\mathbf{Q})=\frac{B}{(\kappa^2+q^{*2})}+\frac{A\kappa}{(\kappa^2+q^{*2})^2}+C\delta(\mathbf{q}^*), \qquad (4)$$

where $\mathbf{q}^*=\mathbf{Q}-\mathbf{q}_{100}$ is the deviation from the Bragg peak position, B is the amplitude of the longitudinal susceptibility, and A is the amplitude of the static longitudinal random-field fluctuations. The normalization of this term is chosen so that as the random field goes to zero and $\kappa\rightarrow0$ as $T\rightarrow T_C$, the Lorentzian squared term evolves into a δ function and the

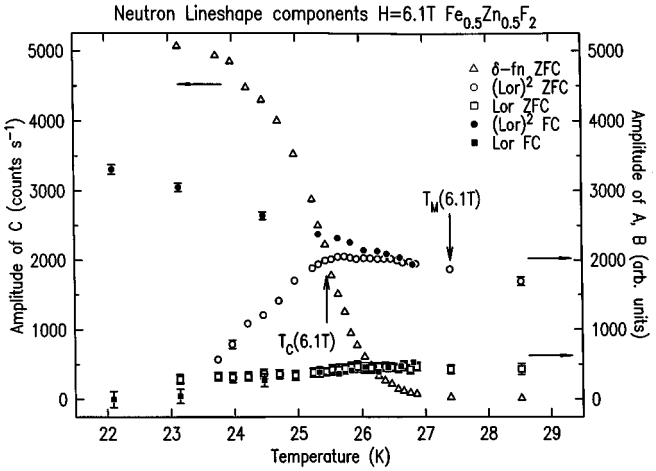

FIG. 7. The temperature dependence of the neutron scattering line shape components as determined by fits to Eq. (4). The long range order (parameter C) is referenced to the left-hand vertical axis. It is constrained to be zero in the FC measurements. The Lorentzian squared fluctuations (parameter A) and Lorentzian fluctuations (parameter B) are referenced to the right-hand vertical scale. Open symbols correspond to ZFC data and closed circles to FC data. The measurements were performed with the spectrometer in the two-axis mode.

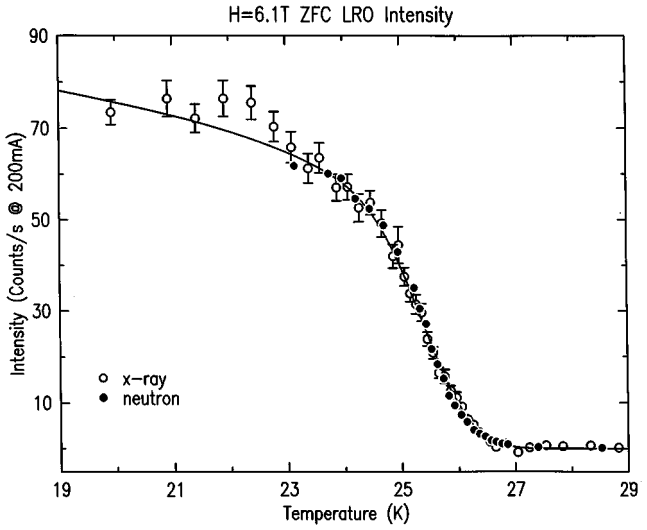

FIG. 8. Neutron and x-ray (100) peak intensities measured at 6.1 T after ZFC. The relative intensities have been adjusted so that they match in the temperature region around $T_C(H)$.

usual Orstein-Zernicke cross section is recovered. The LRO is fitted with the parameter C and the cross section $S(\mathbf{Q})$ is convolved with the full 3D resolution function. An example of the result of such a fit is shown as the solid line in Fig. 6 on a semilog scale. These data were taken at $T=23.1$ K and $H=6.1$ T following a ZFC procedure. The individual components of the line shape are also illustrated.

The temperature dependences of the parameters A, B, and C of Eq. (4) are shown in Fig. 7 under both field-cooled and zero-field-cooled conditions for $H=6.1$ T. Under FC there is no LRO and C is constrained to be zero in these fits (closed symbols). The data are well fit by a Lorentzian squared (L^2) with a small Lorentzian (L) component. The intensity of the L^2 component rises smoothly as the sample is cooled through the metastability boundary. On warming from a ZFC state the data then require $C\neq 0$ in order to fit the LRO. The open symbols in Fig. 7 show the parameters from these fits. These results agree well in their general phenomenology with previous neutron studies on diluted antiferromagnets in an applied field.[15,17,18,22] The metastability boundary, $T_M(H)$, is the point at which the amplitude of the LRO falls to zero. At $H=6.1$ T, $T_M(6.1\text{ T})=27.4\pm 0.3$ K. For $T>T_M(H)$ there are no history dependent effects and the system is in equilibrium. Note $T_M(H)>T_C(H)=25.6$ K. The ZFC diffuse scattering is largely Lorentzian squared in character, indicating that it arises from random-field fluctuations. At $H=6.1$ T the diffuse scattering peak amplitude reaches a maximum intensity ~ 2 K below the metastability boundary.

Extinction effects prevent reliable fitting of the amplitude of the neutron LRO to an order parameter function such as Eq. (3). However, in the transition region, these effects are no longer expected to be significant and here one ought to be able to make a direct comparison of the x-ray and neutron data. Such a comparison is shown in Fig. 8, in which both magnetic x-ray and neutron scattering order parameter measurements at $H=6.1$ T are plotted. These data were taken on the same $Fe_{0.5}Zn_{0.5}F_2$ sample. As previously stated, the neutron data have been shifted by -3.1 K in temperature so that x-ray and neutron scattering measured T_N agrees in zero field, and in fact the data of Fig. 8 serve to illustrate the validity of this procedure. No further adjustment has been made in the temperature scale. The only adjustment then is the rescaling of the neutron intensity by a constant multiplicative factor. As is apparent in Fig. 8, the two sets of data show excellent agreement within 2.5 K of $T_C(6.1\text{ T})$. Thus in the temperature region in which extinction effects do not play a role, the neutron data also display the characteristic rounded power law behavior seen in the x-ray results. The data of Fig. 8 thus confirm that the x-ray results are representative of bulk behavior, and not due to some near-surface effect.

The phenomenology of the transition is clarified in Fig. 9. In the top panel of this figure, the x-ray intensity of the $H=6.1$ T ZFC state is plotted. The solid line is a fit to Eq. (3) with $\beta=0.12$ and $\sigma_{\text{ZFC}}(H=6.1\text{ T})=0.85$ K. The dashed vertical line marks the center of the Gaussian distribution $T_C(H=6.1\text{ T})=25.57\pm 0.02$ K. In the center panel, the width κ of the diffuse scattering, as determined by fits of the neutron data to Eq. (4) at $H=6.1$ T, is plotted for the ZFC and FC data. The closed circles represent the inverse correlation length of the FC domain state which decreases smoothly through the transition, flattening out at low temperatures around $\kappa_{\text{FC}}(H=6.1\text{ T})=0.0075$ reciprocal lattice units. This corresponds to a characteristic length of the FC domain state of ~ 100 Å.

The width, κ of the ZFC diffuse scattering decreases as $T_C(H)$ is approached, but does not go to zero as expected at an equilibrium second order transition. Rather, the correlation length of the fluctuations saturates at $T_C(H)$, at a value approximately equal to the FC length at that temperature. This temperature, at which the largest blocks of spins are being flipped, coincides precisely with the center of the transition region as observed with x rays. It is the point of maximum rate of change of the sublattice magnetization. As the

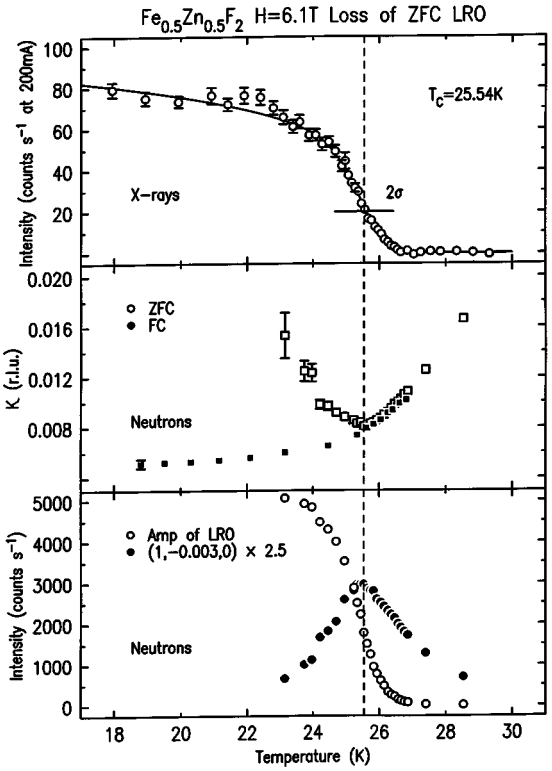

FIG. 9. Top panel: The (100) x-ray magnetic ZFC peak intensity at $H=6.1$ T. The solid line is the result of a fit to the rounded power law, Eq. (3), described in the text. The dashed line represents the center of the distribution at $T_C(6.1\ \mathrm{T})=25.54$ K. Center panel: The inverse correlation length of the diffuse scattering as measured by neutron scattering, with the spectrometer in the double-axis configuration. On field cooling (FC), only a domain state is observed and the data are fit to a Lorentzian plus a Lorentzian squared form: $A/(\kappa^2+q^2)+B\kappa/(\kappa^2+q^2)^2$ (closed circles). The zero-field-cooled (ZFC) data are fit to the same function with the addition of a δ function Bragg peak (LRO) term. The inverse correlation length, κ, is seen to saturate precisely at the temperature of maximal rate of change of the order parameter, $T_C(6.1\ \mathrm{T})$ (open circles). The value at which the correlation length of the ZFC fluctuations saturates is also the FC domain size at that temperature. Bottom panel: The amplitude of the ZFC LRO as measured by neutron scattering (open circles). The closed circles represent the amplitude of the pseudocritical scattering as measured by the intensity of the $(1,-0.003,0)$ reciprocal lattice point. This scattering peaks around $T_C(6.1\ \mathrm{T})$.

temperature is increased further the inverse correlation length begins to increase, following closely the corresponding FC values and the rate of decay of the order parameter falls off.

In the bottom panel of Fig. 9, we plot the amplitude of the LRO (open circles), determined in the neutron scattering measurements, together with the measured neutron intensity at $(1,-0.003,0)$. This position, away from the Bragg peak, provides a measure of the ''critical'' scattering which is independent of any functional form used in the fitting. This pseudocritical scattering also peaks at $T_C(H)$.

The picture of the transition out of the metastable LRO state that emerges then is as follows: At low temperatures, there is very little thermal energy to overcome the random field barriers and only very small blocks of spins flip, to follow their local random fields. As the temperature is raised, the order parameter is reduced through such reversals of the static local magnetization and the transition is approached. As the correlation length grows, the energy barriers corresponding to flipping correlated regions grow at a faster rate and the time scale to relax such fluctuations grows. For an experiment performed in a finite time, the correlation length will appear to saturate at a maximum value. On warming through the transition, the correlation length, and the associated time scale, decrease and the system is once again able to relax on experimental time scales. The system does not attain equilibrium again until all the LRO is removed. This picture is symmetric on warming and cooling, which explains the agreement of the ZFC and FC correlation lengths at $T_C(H)$ and above.

The data presented here are thus in qualitative agreement with the ideas of VF. However, the observed H^2 scaling of the x-ray transition region does not agree with $H^{2/\phi}$ scaling, with $\phi=1.42$, which others have argued for[26] and reported.[22,27] Furthermore, in $Mn_{0.75}Zn_{0.25}F_2$ it has been shown that the broadening is centered about a temperature $T_C(H)$ which is higher than the equilibrium Néel temperature $T_N(H)$. The H^2 field dependence can also be seen in the neutron scattering data. Since the neutron order parameter in this temperature region agrees with those measured with x rays, neutrons will also yield an H^2 dependence. In addition, one can obtain a measure of the width of the transition from measurements of the critical scattering at $(1,-0.003,0)$ as shown in Fig. 10. In Fig. 10(a), the intensity at $(1,-0.003,0)$ is plotted as a function of temperature for a number of fields. The transition is seen to broaden markedly as the applied field is increased. The solid lines are the results of empirical fits to a Lorentzian squared function placed on a flat background which goes linearly to zero above the peak temperature. This form was used without theoretical motivation to parameterize the measured critical scattering and was found to fit the data well at all fields. Other functional forms were also tried and while they did not model the data as well, the same scaling of the widths was seen, independent of the function used. The widths obtained from these fits are then plotted against applied field squared in Fig. 10(b). These data are consistent with a H^2 dependence. A $H^{2/\phi}$ dependence provides a less good description of the data. Interpretation of these widths is somewhat problematical because of the inherent, finite width at $H=0$ T. It has been assumed to add linearly in this analysis. We emphasize that these same critical scattering results are consistent with the known $H^{2/\phi}$ scaling of the phase boundary. That is, a fit of the field dependence of the temperature peak in the critical scattering follows $T_C(H)=T_C(0)-AH^2-BH^{2/\phi}$ with A held fixed at the calculated mean field value, $A=0.0152\ \mathrm{K\,T^{-2}}$, yields $\phi=1.41\pm0.06$. This is in close agreement with the value obtained using birefringence techniques, $\phi=1.40\pm0.05$.[21]

Finally, we note that these neutron results for the transition region width do not agree with previous measurements of a similar kind[22] for which $H^{2/1.42}$ scaling was reported. These latter results were for small fields, $H<3$ T and a zero width was assumed at $H=0$ T.

B. Magnetometry results

In order to make contact with previous measurements of the dynamic rounding by bulk thermodynamic probes, we

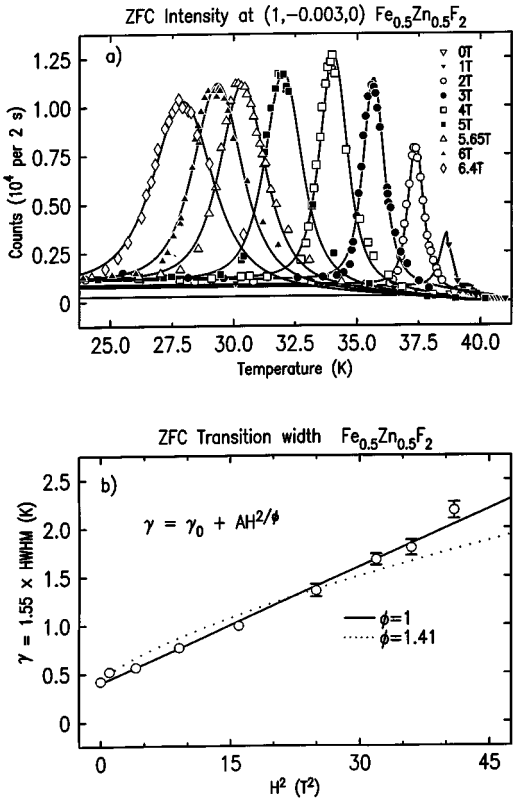

FIG. 10. (a) The ZFC intensity at the (1,−0.003,0) position seen by neutron scattering. The intensity reaches a maximum at $T=T_C(H)$ and occurs at lower temperatures as the field is increased. The peak broadens with increasing field. The solid lines represent empirical fits to a Lorentzian squared function as described in the text. (b) The width of the ZFC transition region as extracted from fits to the data of (a). The temperature width increases linearly with H^2 (solid line). A fit to $H^{2/\phi}$ with ϕ=1.41 is less satisfactory. The zero-field width is assumed to add linearly.

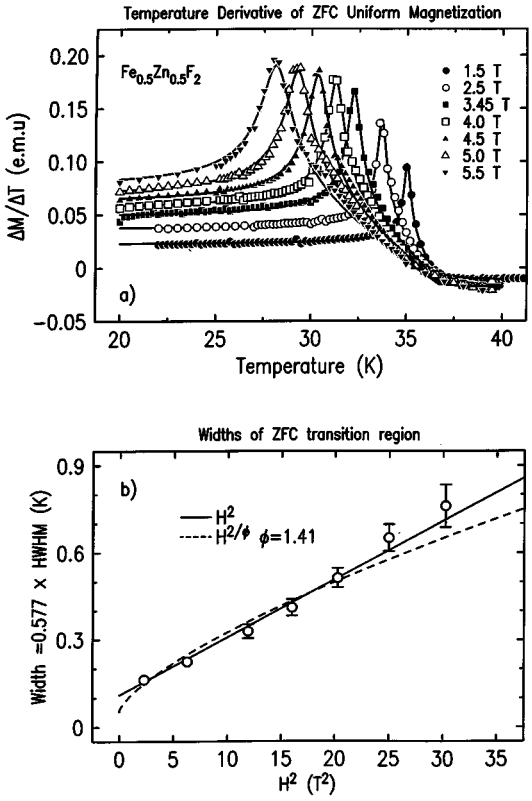

FIG. 11. (a) The temperature derivative of the ZFC *uniform* magnetization as measured by SQUID magnetometry. The transition region is empirically fit by a square root Lorentzian function with a stepped background. (b) The width of the SQUID ZFC transition region extracted from the fits of (a) as a function of H^2. A linear dependence on H^2 (solid line) passes through all the points.

have carried out a series of experiments utilizing a SQUID magnetometer. In an Ising antiferromagnet with the field along the Ising axis, the uniform magnetization, M, provides a measure of the domain wall density. We have performed a set of measurements of the uniform magnetization on a small piece of $Fe_{0.5}Zn_{0.5}F_2$ cut from the same boule as that used in the x-ray and neutron scattering work. Measurements of the FC and ZFC uniform magnetization were made at a number of fields. As discussed by Lederman *et al.*,[32,33] for the FC runs the domain state is evidenced by an excess FC magnetization relative to the ZFC state and $M_{\mathrm{FC}}-M_{\mathrm{ZFC}}>0$. In the present work, we focus on measurements of the ZFC uniform magnetization. The FC state and its time dependence are discussed elsewhere.[24]

One can obtain information on the ZFC transition by measuring the thermal derivative of the uniform magnetization. Previously, workers have interpreted such measurements in terms of equilibrium phenomena. Specifically, taking the scaling form of the equilibrium free energy as $F=|t_H|^{2-\alpha_{\mathrm{REIM}}}f(AH^2/|t_H|^{\phi})$, where $t_H=(T-T_N-BH^2)/T_N$ and assuming a sharp phase transition and random-field behavior within a crossover region, then $f(x)\rightarrow(x-x_0)^{2-\alpha_{\mathrm{RFIM}}}$ is expected.[3] In this region it was argued that the thermal derivative of the uniform magnetization in equilibrium would have a singularity of the form[39]

$$\left(\frac{\delta M}{\delta T}\right)_H \sim H^{(2/\phi)(1+\alpha_{\mathrm{RFIM}}-\alpha_{\mathrm{REIM}}-\phi/2)}[T-T_C(H)]/T_N|^{-\alpha_{\mathrm{RFIM}}}. \tag{5}$$

If $\alpha_{\mathrm{RFIM}}>0$, a divergence would be expected at the equilibrium transition. In fact, recent theory suggests that $\alpha_{\mathrm{RFIM}}=-0.1$,[44] so there should actually be a cusp in equilibrium. We believe that, independent of the question of the applicability of such an equilibrium approach, this analysis is in fact incomplete. In particular, as we discuss in detail below, a LRO contribution should be included. For the moment, we put questions of the interpretation of these data aside; for our current purposes it will be sufficient to obtain a measure of the broadening caused by activated dynamics, in order to compare it with that observed by x-ray and neutron scattering techniques.

In Fig. 11(a), the quantity $(dM/dT)_H$ after zero-field cooling, is plotted for a number of fields. The derivative is calculated from the difference between successive data points, ΔM divided by the temperature interval, ΔT. At low fields a relatively sharp peak is observed. The peak broadens and moves to lower temperatures as the field is increased. The depression in $T_C(H)$ is again consistent with random-field scaling, $H^{2/\phi}$ with ϕ=1.42, although the fit is not unique. In order to make some estimate of the H dependence of the transition broadening, we have modeled these data with a square root Lorentzian, placed on a stepped back-

ground with a linear slope connecting the two levels. Although there is no theoretical justification for this form, the resulting fit is adequate and forms a good basis for parameterization of the empirical results. Fits to this form are shown as solid lines in Fig. 11(a). In Fig. 11(b), the width of the square root Lorentzian is plotted as a function of field. The width of the transition region is again consistent with H^2 scaling (solid line). Finally, we note that since our data are identical to those previously obtained by Lederman *et al.*,[32,33] we conclude that their sample also exhibits the same H^2 scaling. An alternative method of analysis is simply to subtract the FC dM/dT from the ZFC dM/dT. The resultant peak width again scales as H^2. This approach has a solid physical basis, as we discuss later.

As we shall see shortly, this agreement of the x-ray and magnetization measurements of the field scaling of the transition widths is not coincidental and leads to ideas which are useful in interpreting the hysteresis of ZFC and FC protocols observed in indirect heat capacity measurements, such as the thermal derivative of the magnetization. In this phenomenology, the thermal derivative may be described as the sum of two terms, one due to the short range correlations and the other proportional to the derivative of the staggered magnetization squared, dM_s^2/dT. Although we believe that this form provides the correct description of the data, it is important to have an independent test of the H^2 scaling in the logical development of ideas presented below, hence the use of such an empirical description of the data in the preceding analysis.

V. DISCUSSION

A. The scattering results

The broadening of the transition in $Fe_{0.5}Zn_{0.5}F_2$ as observed by x rays is in qualitative agreement with previous x-ray work on $Mn_{0.75}Zn_{0.25}F_2$.[37,36] However, as noted earlier, the broadening in $Fe_{0.5}Zn_{0.5}F_2$ is quantitatively much larger. For an applied field, H, the generated random field, $h_{\rm RF}$, is[4]

$$\langle h_{\rm RF}^2\rangle_{\rm av}=\frac{x(1-x)[T_N^{\rm MF}(1)/T]^2(g\mu_B SH/K_BT)^2}{[1+\Theta^{\rm MF}(x)/T]^2}, \quad (6)$$

where $T_N^{\rm MF}$ (1) is the mean field transition temperature of the pure system and $\Theta^{\rm MF}(x)$ is the mean field Curie-Weiss parameter. For MnF_2 and FeF_2, $\Theta/T_N=1.24$ and 1.48,[45] and $T_N(H=0\ {\rm T})=67$ and 77 K, respectively. For $Mn_{0.75}Zn_{0.25}F_2$, $T_N(H=0\ {\rm T})=46.1$ K and for $Fe_{0.5}Zn_{0.5}F_2$, $T_N(H=0\ {\rm T})=36.7$ K. Assuming $\Theta^{\rm MF}(x)$ scales with the zero field transition temperatures we find the generated random field is $\approx$4 times larger in $Fe_{0.5}Zn_{0.5}F_2$ compared with that in $Mn_{0.75}Zn_{0.25}F_2$ at their respective transition temperatures, $T_C(H=5.0\ {\rm T})$. The observed broadening is $\sim$6 times larger in $Fe_{0.5}Zn_{0.5}F_2$ compared with that in $Mn_{0.75}Zn_{0.25}F_2$ (Ref. 36) at $H=5.0$ T. The effect of the larger random field can also be seen in the inverse correlation lengths of the FC domain state in the two materials. For example at $H=6.1$ T, Fig. 9 shows κ saturating around $\kappa=0.0073$ reciprocal lattice units in $Fe_{0.5}Zn_{0.5}F_2$, whereas at $H=6.5$ T, $\kappa=0.0013$ reciprocal lattice units at low temperatures in $Mn_{0.75}Zn_{0.25}F_2$,[18] a factor of approximately 6 smaller.

As discussed in a previous paper,[36] it is possible to derive empirically the H^2 field dependence. Our present understanding of phase transitions requires that critical phenomena be qualitatively symmetric on both sides of the critical point. One is led to expect that just as extreme critical slowing down prevents the attainment of equilibrium on field cooling, activated dynamics will also operate on warming the ZFC state. Thus as the temperature is raised, the system will fall out of equilibrium, at least on experimentally relevant time scales and the correlation length will saturate, as we observe experimentally. The system will not be able to relax fully until it has passed through the critical region to reach the high temperature equilibrium phase. In Ref. 36, we developed a qualitative picture of the process in which the LRO is destroyed through ''flipping'' of domains with successively larger sizes. The maximum rate of change occurs at the center of the Gaussian distribution which is when the size of the volume being flipped becomes approximately equal to the FC domain size at that temperature. This is demonstrated in Fig. 7. The rounding of the transition may then be understood as a finite size effect in which the growth of the correlation length in the transition region is limited by the random fields to the FC domain size. One then expects the rounding to scale as $\Delta T\sim\xi_{\rm max}^{-1/\nu}$. The inverse correlation length scales with the applied field as $\kappa\sim H^{\nu_H}$. Hence $\Delta T\sim H^{\nu_H/\nu}$. Using the experimentally obtained values, $\nu_H=2.23\pm0.1$ (Ref. 46) at $T=8.0$ K and $\nu=1.0\pm0.15$ (Ref. 47) measured for the $Fe_{1-x}Zn_xF_2$ system, we obtain $\nu_H/\nu=2.23\pm0.7$ in broad agreement with the observed field dependence. For $Mn_{0.75}Zn_{0.25}F_2$ similar agreement was observed; $\nu_H=3.3\pm0.8$, $\nu=1.4\pm0.3$, and $\nu_H/\nu=2.4\pm1.1$.[36] Note that this argument does not require that the system be in equilibrium.

B. Application to indirect specific heat measurements

The detailed results presented above lead to a reinterpretation of indirect specific heat measurements, as discussed in a preliminary report of this work.[13] Specifically, they demonstrate that the transition from the ZFC LRO state is not an equilibrium transition characterized by critical exponents, but rather proceeds via a smooth, rounded power-law decay of the order parameter, and a finite maximum correlation length. We have collectively labeled these phenomena ''*trompe l'oeil*'' critical behavior. This leads to an apparent discrepancy between scattering experiments and bulk thermodynamic probes, such as birefringence and SQUID measurements, since the sharp peak observed in ZFC measurements with these techniques has previously been interpreted as reflecting equilibrium critical behavior, described by a critical exponent $\alpha_{\rm RFIM}$, together with some small dynamic rounding.

Motivated by the similarity between the thermal derivative of the magnetization data and the derivative of the x-ray data scaling function, together with the same field dependence of the transition widths, we argue that in fact the strong hysteresis of the thermodynamic measurements arises from the presence of the nonequilibrium LRO in the ZFC state. Essentially, the hypothesis is as follows: For indirect specific heat measurements, which are based on measuring quantities proportional to the two spin correlation function,

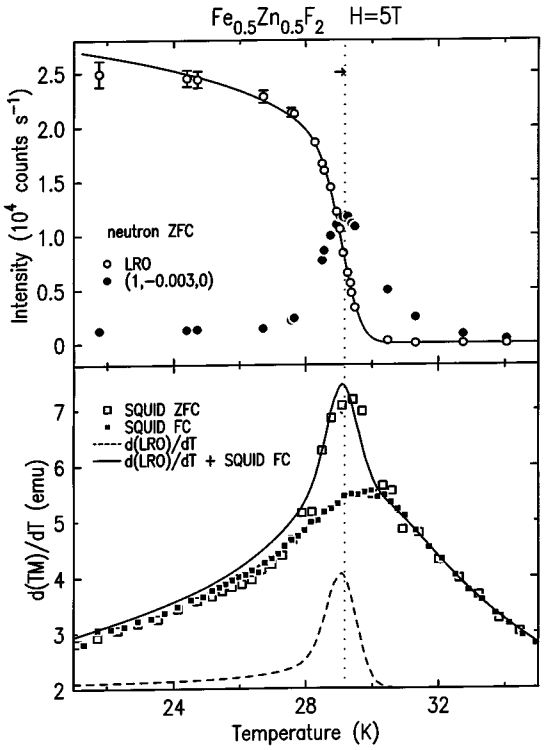

FIG. 12. Top panel: Neutron scattering intensity at (1,0,0) and $(1,-0.003,0)$ at $H=5.0$ T. The solid line is the result of a fit to the rounded power-law dcay of Eq. (3). The small arrow at the top indicates the 0.3 K shift in the neutron data temperature scale. Bottom panel: FC and ZFC data for $d(TM)/dT$ at $H=5.0$ T. The dashed line is the dM_s^2/dT contribution. Only the amplitude has been adjusted. The solid line is the sum of the FC data plus the dM_s^2/dT term.

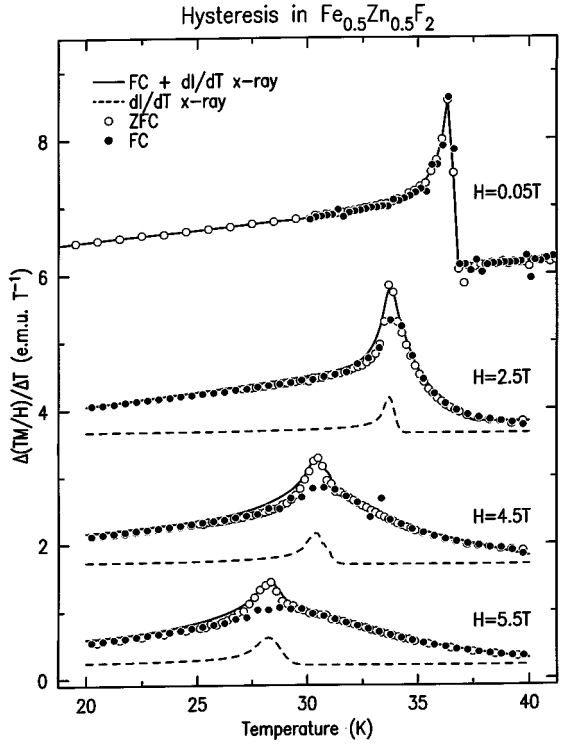

FIG. 13. The temperature derivative of the uniform ZFC and FC susceptibilities, as measured by SQUID magnetometry. The dashed line corresponds to the temperature derivative of the x-ray intensity scaling function, with the intensity scaled to match the difference in the ZFC and FC results. The solid line is the sum of the FC $d(TM/H)/dT$ and $d(M_s^2)/dT$.

there are two contributions to the signal. The first term is proportional to the magnetic energy, arising from the energy fluctuations. The second term is proportional to the staggered magnetization squared M_s^2, the LRO. In a conventional second order transition, $M_s^2 \sim t^{2\beta}$. For derivative measurements this LRO term is typically the stronger singularity for $T<T_N$ and should be especially important in the current case for which the heat capacity fluctuations are not divergent due to the dynamics. Most importantly, the LRO term for RFIM systems will contribute to ZFC but not FC measurements. We make the additional assumption that the fluctuation contribution to $d(TM)/dT$, which is determined by short range correlations, is not very different for FC and ZFC measurements. Therefore, as a first approximation the ZFC $d(TM)/dT$ should be equal to the FC result plus the dM_s^2/dT contribution.

In Fig. 12, we present the results of such analysis for data taken at $H=5.0$ T. In the top panel are the neutron data for the LRO and the $(1, -0.003, 0)$ critical scattering amplitudes. As discussed above, in the transition region the neutron and x-ray order parameter measurements agree precisely. The solid line is the Gaussian power-law decay. In the bottom panel, the magnetization data for ZFC and FC protocols are shown. The temperature scales are normalized so that they agree at zero field. The net accuracy of this normalization is ± 0.3 K. In plotting the data of Fig. 12 we have shifted the neutron data by an additional 0.3 K, as indicated by the small arrow at the top of the figure. This is motivated by the argument that $d(TM)/dT$ should have its maximum at the same temperature for which the correlation length is a maximum.[33] This shift has the additional property of bringing $T_M(H)$ into agreement for the two techniques, a not incidental effect. In any case, we note that the temperature scale shift is within the combined temperature uncertainties. Taking the neutron measurement of M_s^2 (solid line, top panel) and differentiating (dashed line, bottom panel), we add this to the SQUID FC data, resulting in the solid line, bottom panel. Only the amplitude of the dM_s^2/dT contribution has been adjusted. The agreement is compelling.

The utility of such an analysis is further demonstrated in Fig. 13, in which we use the scaling function obtained from the x-ray data to predict the ZFC magnetization data for a series of fields, given the FC data at these fields. Data taken at $H=2.5$, 4.5, and 5.5 T are presented. Again, only the amplitude of the dM_s^2/dT contribution has been adjusted. The width is held fixed at the value obtained from the H^2 scaling law of the x-ray data (Fig. 4). The agreement is very good, especially in light of the simplicity of the approximations used. We emphasize that this procedure requires that the ZFC peak structure arises *solely* from the LRO term and not from critical fluctuations.

In order to test these ideas further, we have carried out direct heat capacity measurements both on samples of $Fe_{0.5}Zn_{0.5}F_2$ taken from the same boule as the samples used in the rest of the work, and on crystals of $Mn_{0.75}Zn_{0.25}F_2$. These will be reported in detail elsewhere.[48] If our ideas are

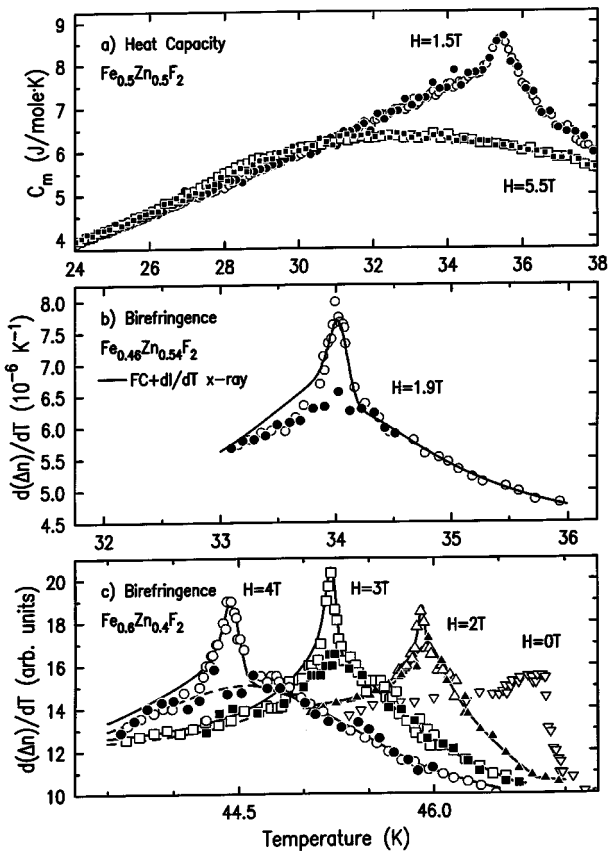

FIG. 14. (a) Heat capacity of $Fe_{0.5}Zn_{0.5}F_2$. There is no evidence of hysteresis on FC and ZFC, nor is there any sign of critical heat capacity in the ZFC data. (b) Optical birefringence data taken from Ferreira, King, and Jaccarino (Ref. 28) for $Fe_{0.46}Zn_{0.54}F_2$. The solid line is the FC data plus the contribution from the $d(M_s^2)/dT$ term. (c) Similar results and analysis for $Fe_{0.6}Zn_{0.4}F_2$ (Ref. 55). In each panel, the open symbols are ZFC data and the closed symbols are FC results.

correct, then direct heat capacity, which is sensitive to the local spin configuration and not to the LRO, should show little hysteresis. In the top panel of Fig. 14, we display direct heat capacity data taken on $Fe_{0.5}Zn_{0.5}F_2$ at $H=1.5$ T, and 5.5 T. These data were taken using a semiadiabatic technique described elsewhere.[48] The time scale for each datum point is $\sim$20 s. There is no observable hysteresis in either data set. This demonstrates that the FC and ZFC fluctuations are closely similar. It is clear that the ZFC peak of indirect heat capacity methods is not indicative of the true heat capacity. The measurements on $Mn_{0.75}Zn_{0.25}F_2$ (Ref. 48) also showed no hysteresis in agreement with previously published work on $Mn_{0.5}Zn_{0.5}F_2$.[49,50] However, hysteresis in the heat capacity of $Fe_{0.46}Zn_{0.54}F_2$ in a field has been reported.[51] We cannot explain this latter result.

Given the success of this approach, it is natural to ask if there is any theoretical justification for the inclusion of a LRO term for indirect heat capacity measurements. In fact, a number of authors have discussed the presence of such a term, although no rigorous theory applicable to diluted antiferromagnets in a field exists. Fisher and Langer first noted the presence of the LRO term for $T<T_C$ in resistive measurements of the specific heat, via $d\rho/dT$.[52] In the random field context, Fishman and Aharony[3] argued that there is a term like M_s^2 in the uniform susceptibility at $H=0$ T, which sums to zero in the case of pure systems. (Note, this term, which arises from the bond disorder has not been seen experimentally. It is not the term we see, which goes to zero at $H=0$ T, and arises from the random fields.) Also Wong[53] has speculated that indirect specific heat measurements contain an additional singularity in nonzero fields arising from the disconnected part of the correlation function, present for diluted systems. Finally, for birefringence measurements in good Ising systems, Ferre and Gehring showed that $\Delta n^{zx} \sim \Sigma_r g(r)\langle S_0^z S_r^z\rangle \sim AU + BM_s^2$, where U is the magnetic energy and $B=0$ only under certain conditions.[54] In line with these arguments, we expect that on general grounds one can argue that all such indirect specific heat measurements may contain a LRO term unless it is symmetry forbidden; they are each $q=0$ measurements of bulk phenomena and are sensitive to the global spin configuration, not just the local one. It may be the case that the LRO term cancels under certain particular conditions, for instance in zero field, but it is clear that this will not necessarily be true in general.

Following such logic, we have tested these ideas on published birefringence data, as shown in the bottom two panels of Fig. 14. In Fig. 14(b), we show data of Ferreira *et al.*[28] taken on a sample of $Fe_{0.46}Zn_{0.54}F_2$ of very high quality. In this case, the solid line is the x-ray scaling function with the width taken from the H^2 scaling law which we have determined here for our $Fe_{0.5}Zn_{0.5}F_2$ sample and with the $H=0$ T width taken to be zero, to account for the higher quality crystal. The FC data are used for the background arising from the noncritical fluctuations. $T_C(H)$ was adjusted slightly from the value determined in our experiments on $Fe_{0.5}Zn_{0.5}F_2$. Again the agreement is good. Finally, in Fig. 14(c) we show similar data[55] and analysis for $Fe_{0.6}Zn_{0.4}F_2$. In this case, the coefficient of the H^2 width is fitted at $H=4$ T. Once more the model describes the ZFC birefringence data well.

VI. SUMMARY

We have studied the transition out of the LRO ZFC state in the strongly anisotropic diluted antiferromagnet $Fe_{0.5}Zn_{0.5}F_2$ in applied fields up to $H=7.0$ T. Using the technique of magnetic x-ray scattering, the order parameter was observed to decay with a continuous power-law-like transition with an average exponent, $\beta_{\rm ZFC}=0.15\pm0.05$. The transition is rounded and this was modeled by a Gaussian distribution of transition temperatures, centered at $T_C(H)$ with a HWHM$=0.83\sigma_{\rm ZFC}(H)$. $\sigma_{\rm ZFC}(H)$ was found to be proportional to H^2, contrary to the previously reported field dependence of $H^{2/\phi}$ with $\phi=1.41$.[22] Using double axis neutron scattering, the diffuse component of the scattering below the transition was observed. The width of the diffuse scattering was found to reach a minimum at $T_C(H)$, but it does not go to zero as would be expected at an equilibrium second order transition. The rounding is believed to be caused by anomalously slow dynamics resulting from the presence of the multiple minima in the free energy. Using finite size arguments and empirical scaling relations for the correlation length we obtain $\sigma_{\rm ZFC} \sim H^{2.2\pm0.7}$ in approximate agreement with experiment. In addition, the width of the transition was measured from the temperature width of the peak in the neutron critical

scattering and from the thermal derivative of the uniform magnetization. Both display an $\sim H^2$ dependence.

The ZFC results presented here in $Fe_{0.5}Zn_{0.5}F_2$ are essentially identical to those observed previously in $Mn_{0.75}Zn_{0.25}F_2$ (Refs. 36 and 37) except, as noted above, for the magnitude of the rounding of $T_C(H)$. Accordingly, our interpretation coincides with that previously given for the Mn system. Specifically, the observed pseudocritical behavior simulates ordinary critical phenomena at a second order transition, but in fact explicitly represents escape from metastability. We previously labeled this ''*trompe l'oeil*'' critical behavior. Thus $T_C(H) > T_N(H)$ where the latter is the true (hidden) equilibrium Néel transition temperature. The diminution of the order parameter and the associated fluctuations studied here occur entirely in the temperature region above $T_N(H)$. No true phase transition after ZFC occurs at $T_N(H)$ because of the pathologically slow dynamics. The progressively larger rounding observed with increasing field can be described as a finite size effect due to the random fields limiting the largest domain that can be flipped. Using neutron diffraction we have observed these nonequilibrium local fluctuations directly. We note that this interpretation differs from that given in many previous studies of ZFC behavior in $Fe_{1-x}Zn_xF_2$, for example, Refs. 21, 22, and 25–29. In these papers, the ZFC behavior is interpreted as largely reflecting the true equilibrium critical behavior of the RFIM with the addition of a relatively small amount of dynamic rounding. Our results lead us to believe that there is no equilibrium phase transition after zero-field cooling and that dynamic effects dominate. We emphasize that the data presented here and those reported in Refs. 21, 22, and 25–29 are entirely consistent with each other; only the interpretations differ.

This apparent discrepancy of interpretations led us to reexamine indirect specific heat measurements which display a marked peak on warming from a ZFC state and, as mentioned, had previously been interpreted in terms of critical specific heat with $\alpha_{\mathrm{RFIM}} \approx 0$. We postulated that the hysteresis in fact arises from a LRO contribution to the signal, and that this may be a general feature of these techniques. Taking the thermal fluctuations in the ZFC and FC state to be similar, we are then led to the prediction that the ZFC data are the sums of the FC fluctuations and a LRO piece which may be derived from our x-ray measurements. Good agreement with both our own SQUID magnetization data and published birefringence data was found when the data were modeled in this way. In this picture, the ZFC peak of indirect heat capacity measurements arises solely from the decay of the LRO and not from critical fluctuations. This is confirmed by our direct heat capacity measurements which show neither a critical contribution nor measurable hysteresis. A rigorous theoretical basis for this approach is now called for. In particular, predictions for the field dependence of any LRO contribution and for an analytical form for the order parameter decay are required and could be tested empirically.

Finally, we note that the experimental results on $Fe_{0.5}Zn_{0.5}F_2$ presented in this paper illustrate the power of combining magnetic x-ray and neutron scattering as well as bulk magnetization techniques to study this complex problem.

ACKNOWLEDGMENTS

It is a pleasure to acknowledge stimulating discussions with A. Aharony, M. Lederman, R. Orbach, M. Schwartz, and P. Z. Wong. We also thank T. R. Thurston for his invaluable assistance with the neutron portion of this work. The work at Brookhaven National Laboratory was carried out under Contract No. DE-AC02-76CH00016, Division of Materials Science, U.S. Department of Energy. The work at MIT was supported by the NSF under Grant No. DMR 93-15715.

*Present address: Lightening Optical Corporation, 431 East Spruce St., Tarpon Springs, FL 34689.

[1] J. Z. Imbrie, Phys. Rev. Lett. **53**, 1747 (1984).
[2] J. Z. Imbrie, Commun. Math. Phys. **98**, 145 (1985).
[3] S. Fishman and A. Aharony, J. Phys. C **12**, L729 (1979).
[4] J. L. Cardy, Phys. Rev. B **29**, 505 (1984).
[5] P. Z. Wong, S. von Molnar, and P. Dimon, Solid State Commun. **48**, 573 (1983).
[6] R. J. Birgeneau, R. A. Cowley, G. Shirane, and H. Yoshizawa, Phys. Rev. Lett. **54**, 2147 (1985).
[7] J. Villain, J. Phys. (France) **46**, 1843 (1985).
[8] D. S. Fisher, Phys. Rev. Lett. **56**, 416 (1986).
[9] A. Aharony, Y. Imry, and S. Ma, Phys. Rev. Lett. **37**, 1364 (1976).
[10] A. R. King, J. A. Mydosh, and V. Jaccarino, Phys. Rev. Lett. **56**, 2525 (1986).
[11] A. E. Nash, A. R. King, and V. Jaccarino, Phys. Rev. B **43**, 1272 (1991).
[12] D. A. Huse, Phys. Rev. B **36**, 5383 (1987).
[13] R. J. Birgeneau, Q. Feng, Q. J. Harris, J. P. Hill, A. P. Ramirez, and T. R. Thurston, Phys. Rev. Lett. **75**, 1198 (1995).
[14] D. P. Belanger, Phase Transit. **11**, 53 (1988).
[15] R. J. Birgeneau, R. A. Cowley, G. Shirane, and H. Yoshizawa, J. Stat. Phys. **34**, 817 (1984).
[16] D. P. Belanger and A. P. Young, J. Magn. Magn. Mater. **100**, 272 (1991).
[17] R. A. Cowley, R. J. Birgeneau, and G. Shirane, Physica (Amsterdam) A **140**, 285 (1986).
[18] R. A. Cowley, G. Shirane, H. Yoshizawa, Y. Uemura, and R. J. Birgeneau, Z. Phys. B **75**, 303 (1989).
[19] R. A. Cowley, H. Yoshizawa, G. Shirane, M. Hagen, and R. J. Birgeneau, Phys. Rev. B **30**, 6650 (1984).
[20] R. J. Birgeneau, Y. Shapira, G. Shirane, R. A. Cowley, and H. Yoshizawa, Physica B **137**, 83 (1986).
[21] D. P. Belanger, A. R. King, V. Jaccarino, and J. L. Cardy, Phys. Rev. B **28**, 2522 (1983).
[22] D. P. Belanger, V. Jaccarino, A. R. King, and R. M. Nicklow, Phys. Rev. Lett. **59**, 930 (1987).
[23] D. P. Belanger *et al.*, J. Magn. Magn. Mater. **140-144**, 1549 (1995).
[24] Q. Feng, J. P. Hill, R. J. Birgeneau, and T. R. Thurston, Phys. Rev. B **51**, 15 188 (1995).
[25] U. A. Leitao and W. Kleenman, Phys. Rev. B **35**, 8696 (1987).
[26] C. A. Ramos, A. R. King, and V. Jaccarino, Phys. Rev. B **37**, 5483 (1988).
[27] P. Pollack, W. Kleenman, and D. P. Belanger, Phys. Rev. B **38**, 4773 (1988).
[28] I. B. Ferreira, A. R. King, and V. Jaccarino, Phys. Rev. B **43**, 10 797 (1991).

[29] S-J. Han, D. P. Belanger, W. Kleenmann, and U. Nowak, Phys. Rev. B **45**, 9728 (1992).
[30] Y. Shapira and N. F. Oliveira, Phys. Rev. B **27**, 4336 (1983).
[31] Y. Shapira, N. F. Oliveira, and S. Foner, Phys. Rev. B **30**, 6639 (1984).
[32] M. Lederman, J. V. Selinger, R. Bruinsma, J. Hammann, and R. Orbach, Phys. Rev. Lett. **68**, 2086 (1992).
[33] M. Lederman, J. V. Selinger, R. Bruinsma, R. Orbach, and J. Hammann, Phys. Rev. B **48**, 3810 (1993).
[34] J. C. Sartorelli, Phys. Rev. B **45**, 10 779 (1992).
[35] J. P. Hill, T. R. Thurston, M. J. Ramstad, R. W. Erwin, and R. J. Birgeneau, Phys. Rev. Lett. **66**, 3281 (1991).
[36] J. P. Hill, Q. Feng, R. J. Birgeneau, and T. R. Thurston, Z. Phys. B **92**, 285 (1993).
[37] J. P. Hill, Q. Feng, R. J. Birgeneau, and T. R. Thurston, Phys. Rev. Lett. **70**, 3655 (1993).
[38] T. R. Thurston, C. J. Peters, R. J. Birgeneau, and P. M. Horn, Phys. Rev. B **37**, 9559 (1988).
[39] W. Kleenman, A. R. King, and V. Jaccarino, Phys. Rev. B **34**, 479 (1986).
[40] A. T. Ogielski and D. A. Huse, Phys. Rev. Lett. **56**, 1298 (1986).
[41] M. T. Hutchings, B. D. Rainford, and H. J. Guggenheim, J. Phys. C **3**, 307 (1970).
[42] G. Jug, Phys. Rev. B **27**, 609 (1983).
[43] P. Z. Wong, Phys. Rev. Lett. **77**, 2338 (1996); and P. Z. Wong (private communication).
[44] M. Gofman, J. Adler, A. Aharony, A. B. Harris, and M. Schwartz, Phys. Rev. Lett. **71**, 1569 (1993).
[45] C. Kittel, *Introduction to Solid State Physics* (Wiley, New York, 1986).
[46] R. A. Cowley, H. Yoshizawa, G. Shirane, and R. J. Birgeneau, Z. Phys. B **58**, 15 (1984).
[47] D. P. Belanger, A. R. King, and V. Jaccarino, Phys. Rev. B **31**, 4538 (1985).
[48] Q. Feng, R. J. Birgeneau, and A. P. Ramirez (unpublished).
[49] H. Ikeda and K. Kikuta, J. Phys. C **17**, 1221 (1984).
[50] H. Ikeda, J. Phys. C **19**, L811 (1986).
[51] K. E. Dow and D. P. Belanger, Phys. Rev. B **39**, 4418 (1989).
[52] M. E. Fisher and J. S. Langer, Phys. Rev. Lett. **13**, 665 (1968).
[53] P. Z. Wong, Phys. Rev. B **34**, 1864 (1986).
[54] J. Ferre and G. A. Gehring, Rep. Prog. Phys. **47**, 513 (1984).
[55] I. B. Ferreira, Ph.D. thesis, UCSB, Santa Barbara, CA, 1992.